Dramatic Enhancement of High-Order Harmonic Generation

Eiji J. Takahashi,[1,*] Tsuneto Kanai,[1] Kenichi L. Ishikawa,[2,3] Yasuo Nabekawa,[1] and Katsumi Midorikawa[1]

[1]*Laser Technology Laboratory, RIKEN, 2-1 Hirosawa, Wako, Saitama 351-0198, Japan*

[2]*Department of Quantum Engineering and Systems Science, Graduate School of Engineering, University of Tokyo, Hongo 7-3-1, Bunkyo-ku, Tokyo 113-8656, Japan*

[3]*PRESTO (Precursory Research for Embryonic Science and Technology), Japan Science and Technology Agency, Honcho 4-1-8, Kawaguchi-shi, Saitama 332-0012, Japan*

(Received 15 October 2006; published 2 August 2007)

We present a dramatic enhancement [Phys. Rev. Lett. **91**, 043002 (2003)] of high-order harmonic generation by simultaneous irradiation of booster harmonics. A key feature of our experiment is the use of mixed gases (Xe and He) with different ionization energies. The harmonics from Xe atoms act as a booster to increase the harmonic yield from He by a factor of 4×10^3. The dominance of the dramatic enhancement effect is supported by simulation with the time-dependent Schrödinger equation as well as the observed spatial characteristic of the generated harmonics and dependence on medium conditions.

DOI: 10.1103/PhysRevLett.99.053904 PACS numbers: 42.65.Ky, 32.80.Rm, 42.50.Hz

High-order harmonic generation (HHG) has been recently recognized as one of the best methods of producing an ultrashort coherent light source covering a wavelength range from the vacuum ultraviolet (VUV) region to the soft x-ray region. High-order harmonics (HH) sources have successfully opened new research areas, such as attosecond science [1,2] and nonlinear optics in the XUV region [3,4]. Attosecond pulses from HHG allow us to study ultrafast inner-shell dynamics directly [5]. The nonlinear process induced by intense XUV fields is also a very attractive phenomenon, enabling one to directly measure the pulse duration of attosecond XUV pulses [6–8]. These new fields are expected to reveal new features of the interaction between electrons and photons.

The generation of a single attosecond pulse (SAP) as well as an attosecond pulse train (APT) based on HHG have been reported. Both SAP and APT will play a pivotal role in the study of ultrafast electron dynamics. In this context, new applications of combined infrared (IR) lasers and SAP and/or APT fields have been proposed theoretically, such as strong-field quantum path control [9], attosecond control of ionization and HHG [10], and dramatic enhancement (DE) of HHG [11–13]. These novel processes enable us to manipulate the time-frequency characteristics of HHG at the single atom level. In particular, the DE is an attractive phenomenon because it may be crucial for the further development of a high-efficiency HH light source [14].

The general feature of HHG can be explained by a three-step model [15]. The basic idea of the DE is that the rate of tunneling ionization, the first step of the model, is boosted by the simultaneous irradiation of the XUV field with the driving IR laser field for harmonic generation because XUV photons promote a transition to virtual states, which significantly reduces the tunneling barrier. The theoretical calculation predicts that the harmonic yield can be enhanced by many orders of magnitude compared with the case of the fundamental pulse alone [11–13]. The first experimental report of the enhancement of HH describes the measurement of HH at around 90 eV in He using a combination of XUV HH generated in a Xe-filled capillary and an IR laser pulse [16,17]. The measured increase in the HH yield was only a factor of 3. It was explained that the conditions required for the DE process, such as interaction geometry, optimum time delay, interaction volume, and phase matching (PM) , were not satisfactorily fulfilled in the experiment. Thus, it was concluded that the observation of the increase in the HH yield might not be due to the DE process but simply attributed to the increase in the interaction volume for the harmonic emission with an aid of the XUV field.

In this Letter, we report on experimental evidence of the DE process. A key strategy of our experiment is the use of a mixture of two kinds of rare gases as the harmonic emission medium, instead of the two-step schemes originally considered in Refs. [11,12] and used in Refs. [16,17]. The mixed-gas target contains He and Xe atoms. Because of a large difference in their ionization potentials, when a pump pulse is focused in the mixed gas, it is neutral Xe atoms that predominantly emit up to the 23rd XUV harmonic, which subsequently boosts the harmonic generation of higher orders from He atoms, together with the incident IR pulse. We call the harmonic generated from Xe atoms the ''booster Xe HH'' or simply ''booster HH,'' hereafter. This method has many advantages, such as easy alignment, a good matching of the interaction volumes, the utilization of high-intensity HH without XUV optics, and the suppression of booster HH absorption. The enhancement factor as compared with a gas containing only He is measured to be 4×10^3 at the 27th harmonic, and the observed spatial characteristic of the HH beam also supports the fact that the DE process is actually occurring. The experimental results agree well with the results of a direct numerical solution of the three-dimensional time-dependent Schrödinger

equation (TDSE). In addition, we measure the harmonic yield under different medium conditions with the aim of optimizing the output performance. While the dependence of the optimum pressure on the mixing ratio indicates that the PM is achieved, that of the harmonic intensity reveals that the DE is a dominant enhancement mechanism.

The experiment was carried out using a 10 Hz Ti:sapphire laser system. In this system, the pulse width was 30 fs and the wavelength was centered at 800 nm. The pump pulse was loosely focused to an interaction cell using an $R = 10$ m concave mirror. We set the focusing point at the entrance pinhole of the interaction cell, and the mixed gas was statically filled in the cell. The medium length was fixed to be 120 mm. The spot size ($1/e$ radius) of the pump pulse at the focus was estimated to be 210 μm with an attenuated pump pulse having a beam diameter of 20 mm. Thus, the Rayleigh length was calculated to be over 170 mm. The pump energy was set at 15 mJ. The generated harmonics were measured by the spectrometer. Details of our HHG experimental setup have been presented in a previous publication [18]. Here, we define the mixing ratio η of the target gas as $\eta = P_{\mathrm{Xe}}/P_{\mathrm{He}}$, where P_{He} and P_{Xe} are gas pressures of He and Xe, respectively. The total gas pressure P is expressed as $P = P_{\mathrm{He}} + P_{\mathrm{Xe}} = P_{\mathrm{He}}(1 + \eta)$.

In Fig. 1(a), we show the experimentally obtained harmonic spectrum of the mixed gas with a 4000-Å-thick Al filter. To generate the booster Xe HH effectively [18], the interaction intensity was fixed at $I_0 = 1 \times 10^{14}$ W/cm^2. That effective interaction intensity I_0 was derived from the Ar HH spectrum [14]. Note that the self-focusing does not occur, since the target gas pressure is sufficiently low. The mixed-gas conditions are as follows: $\eta = 0.04$, $P \sim 8$ Torr, $P_{\mathrm{He}} = 7.68$ Torr, and $P_{\mathrm{Xe}} = \eta P_{\mathrm{He}} = 0.31$ Torr. For comparison, we also show the harmonic spectra with the Al filter obtained when the target gas contains only Xe ($P_{\mathrm{Xe}} = 0.31$ Torr) or He ($P_{\mathrm{He}} = 7.68$ Torr). The Al filter was used to reduce the radiation longer than 80 nm. According to the three-step semiclassical model [15], the highest harmonic energy, the cutoff energy, is given by $I_p + 3.17U_p$, where U_p is the ponderomotive energy and I_p is the atomic ionization potential. At an intensity of 1×10^{14} W/cm^2, the cutoff energy is calculated to be 31.1 eV ($\sim$ H21) for Xe and 43.5 eV ($\sim$ H29) for He. Thus, the 27th to 35th harmonics, observed only with the mixed gas, are emitted from He atoms. On the other hand, virtually no harmonic signal can be seen for the He gas, since the harmonic efficiency is very low owing to its large ionization potential (24.6 eV). This indicates that HHG from He atoms is dramatically enhanced by the presence of Xe atoms. The large background noise in the Xe spectrum was due to the scattering of lower-order harmonics in the spectrometer because the spatial distribution of the noise observed using the two-dimensional spectrometer is clearly different from the harmonic signals of the 23rd to 33rd orders. However, we could not precisely determine

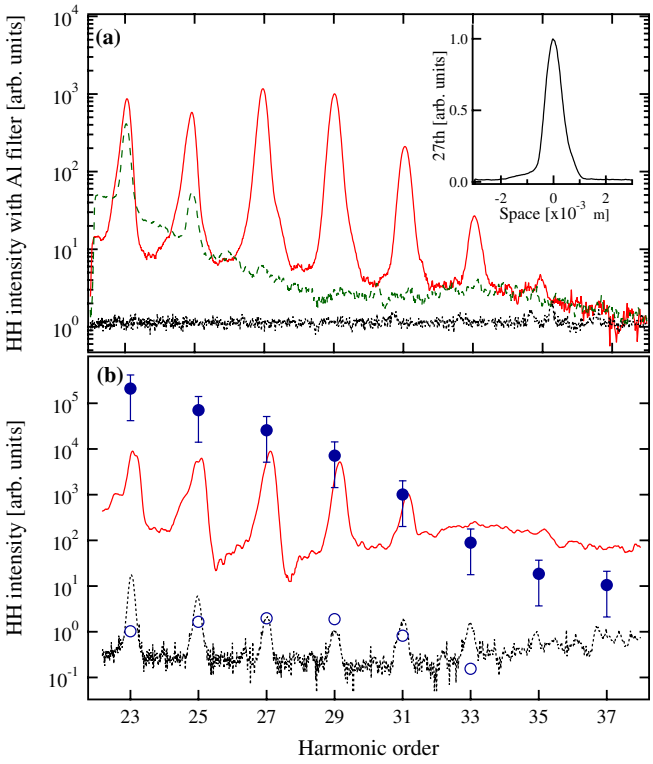

FIG. 1 (color online). Experimentally obtained harmonic spectra (a) with and (b) without Al filter from the mixed gas (solid line), He (dotted line), and Xe (dashed line). The inset shows the measured far-field spatial profile of the 27th harmonic in 8 Torr $\eta = 0.04$ mixed gas. Open and solid circles show the intensity of numerical results in He HHG and DE HHG, respectively.

the amplified gain by the DE process in Fig. 1(a). To directly compare the signal strength with and without the DE process, we removed the Al filter. The results are shown in Fig. 1(b). As discussed above, crucial evidence of the DE is expected to appear at harmonic orders higher than the 25th order for the He-Xe mixed target gas, while the lower harmonics contain the contribution from Xe atoms. The experimental cutoff energies of He and Xe in Fig. 1 are roughly in agreement with the above-mentioned values. The larger scattered noise from the Xe was strongly absorbed by the He gas in the case of the mixed gas. Comparing the HH spectra obtained using the He gas and the mixed gas, the harmonic amplified gain by the DE was determined to be 4×10^3 at the 27th HH. The net output flux of DE around 45 eV was lower than that of the optimized Ar PM condition [14] in same interaction intensity. This is because the Ar gas has large atomic polarizability, compared with He gas. The DE is particularly effective when the pump pulse alone hardly ionizes the target gas.

The inset in Fig. 1(a) shows the far-field spatial profile of the 27th HH in the 8 Torr mixed gas ($\eta = 0.04$). The output beam divergence was measured to be 0.4 mrad FWHM with a Gaussian profile, while the divergence angle in only He gas was 0.65 mrad FWHM. From those measured values, the spot sizes at the interaction cell were

estimated to be ~30 μm for the mixed gas and ~20 μm for He on the basis of the diffraction of the Gaussian beam. Thus, the spot size of the H27 in the mixed gas is larger than that in the He gas. This can be explained by the DE mechanism as follows. Since the dependence of the tunneling ionization rate on the laser intensity is highly nonlinear, HHG in the He gas is spatially confined to a small area around the beam axis. In contrast, in the DE of HHG, the initial step in the three-step model, i.e., the tunneling ionization, is assisted by a single XUV photon absorption of booster Xe HH. Since the single photon absorption is a linear process in contrast to tunneling ionization, the DE becomes marked, particularly in the low-intensity region of the pump pulse where tunneling hardly occurs. This leads to the DE HHG in a much larger volume. As a result, the spot size becomes larger for the mixed gas than for the He gas. Our observations clearly support the characteristics of the DE process.

To reinforce our understanding of the DE scenario in the mixed gas, we compare the experimental data with the results of direct numerical solution of the TDSE in the single-active-electron (SAE) approximation,

$$i\frac{\partial\psi(\mathbf{r},t)}{\partial t} = \left[-\frac{1}{2}\nabla^2 + V(r) + z[E_f(t) + E_h(t)]\right]\psi(\mathbf{r},t), \quad (1)$$

with an effective potential [19,20] for He, $V(r) = -(1 + e^{-Br})/r$, $B = 2.505$, which faithfully reproduces the eigenenergies of the ground and the first excited states. $E_f(t)$ is a fundamental optical field, and the booster harmonic field $E_h(t)$ from Xe is constructed using the experimentally obtained intensity of the 11th to 23rd harmonics [18] with the relative phases determined from the three-step model [15], since the booster HH constructs the APT [7]. The total amount of booster HH intensity of the 11th to 23rd harmonics in the mixed gas is $\sim 1 \times 10^{11}$ W/cm^2, and is typically 8×10^9 W/cm^2 at the 15th harmonic, where the pulse width of the booster HH is assumed to be the same as that of the pump pulse, and the spot size at the interaction region is estimated from the measured HH beam divergence. The contribution of the harmonics lower than the 11th harmonic is negligible, as discussed below. The DE harmonic spectrum from He is obtained by a Fourier transform of the time-dependent dipole acceleration.

Filled and open circles in Fig. 1 present the calculated harmonic spectra with and without the booster HH, respectively. The error bars of filled circles stand for the uncertainty of the booster HH intensity between 10^{10} and 10^{11} W/cm^2. The results are normalized at the H27 without the booster. The calculated values are in agreement with the experimental results. The remaining difference might be explained by macroscopic effects, e.g., absorption, PM, and volume effects. The booster field $E_h(t)$ in the present simulations does not include the contribution of the harmonics lower than the 11th harmonic, whose intensity could not be measured in our experimental setup. To check whether these harmonic components affect the DE process, we performed a simulation including H9, assuming that its intensity is the same as that of H11 and found that the result remains practically unchanged. The mechanism of the DE can be interpreted as tunneling from a virtual state [11,12], whose nominal ionization potential is defined as 24.6 eV-$q\hbar\omega_0$, where q denotes the order of the booster harmonic and ω_0 is the fundamental frequency. The corresponding Keldysh parameters [21] indicate that the ionization from the virtual state belongs to the tunneling regime only for $q \geq 11$. Thus, the efficiency of the DE process by the 11th to 23rd harmonics is 3 orders of magnitude higher than that by harmonics lower than the 11th.

As the next step, we measured the HH yield under several medium conditions to optimize the output performance and clarify the role of PM. We chose the target gas pressure P and the mixing ratio η as the variable parameters. P exerts a great influence upon the PM, whereas η determines the booster Xe HH intensity. Figure 2 shows the gas pressure optimized for H27 as a function of the mixing ratio η at a focusing intensity of 1×10^{14} W/cm^2 and a medium length L_{med} of 12 cm. The optimized gas pressure decreases as the mixing ratio increases. This dependence is explained by considering the standard PM model [18,22,23], as follows.

The amplitude A_q of the qth harmonic taking into the absorption effect of the medium is given by $A_q = N_0 d(q\omega_0) \times \exp(i\pi z/L_{\text{coh}})\exp[-(L_{\text{med}} - z)/(2L_{\text{abs}})]dz$, where $L_{\text{coh}} = \pi/\Delta k$ is the coherence length with $\Delta k = k_q - qk_0$ being the total phase mismatch between the HH field and the atomic dipole, and L_{abs} is the absorption length for the given harmonic. Even when L_{coh} ($\Delta k \sim 0$) is infinite, the HH emission saturates as soon as L_{med} is longer than $3L_{\text{abs}}$. In a loosely focusing geometry of the pump pulse, the Gouy phase (k_{gouy}), the negative dispersion (k_{neu}), and

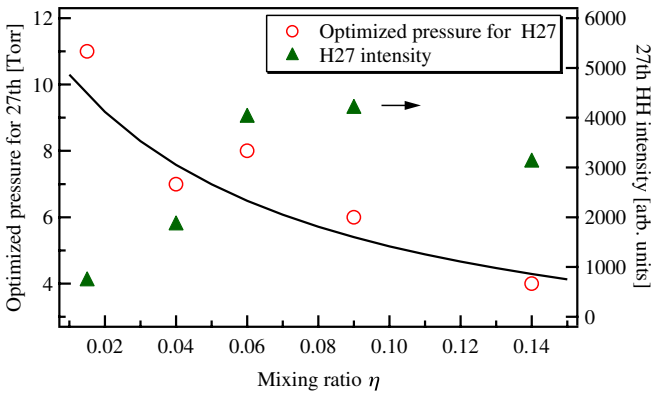

FIG. 2 (color online). Optimized gas pressure for the 27th harmonic and the maximum 27th harmonic intensity as a function of mixing ratio. The solid line shows the calculated optimized mixing ratio under the PM condition in a mixed gas target.

the plasma dispersion (k_{fe}) of the medium are the PM factors. The Gouy phase k_{gouy} at the interaction point is estimated to be $5.85 \times 10^{-2} q\ \mathrm{cm}^{-1}$ from the measured spot size of the pump pulse. The dispersion of the mixed gas is expressed as $k_{\mathrm{neu}} = -0.8 \times (P_{\mathrm{Xe}} f_{1\mathrm{Xe}} + P_{\mathrm{He}} f_{1\mathrm{He}})/q - 103q \times (6.38 \times 10^{-4} P_{\mathrm{Xe}} + 3 \times 10^{-5} P_{\mathrm{He}})$, where f_1 is the atomic scattering coefficient. In addition, the plasma dispersion k_{fe} is given by $0.73 q P_{\mathrm{He}}(\eta\gamma_1 + \gamma_2)$, where γ_1 and γ_2 correspond to the ionization rate of Xe and He, respectively. In our experimental pump intensity, since the He gas is perfectly neutral condition ($\gamma_2 \approx 0$), the amount of ionization rate in the mixed gas is determined by the ionization rate (γ_1) of Xe gas. The ionization rate of the Xe gas attains $\gamma_1 \sim 0.3$, which calculated by Ammosov-Delone-Krainov (ADK) ionization theory [24]. Under the optimized PM condition ($\Delta k = k_{\mathrm{gouy}} + k_{\mathrm{fe}} - k_{\mathrm{neu}} \sim 0$) for H27, the relation between the mixing ratio (η) and the gas pressure (P) , shown as a solid curve in Fig. 2, is in good agreement with the experimental results. Moreover, we obtained a low-divergence beam with a Gaussian beam profile. This good beam quality indicates that the PM condition is substantially satisfied on the propagation axis of the pump pulse.

Filled triangles in Fig. 2 show the net H27 signal under the phase-matched condition as a function of the mixing ratio η. It first increases with an increasing value of η and reaches its maximum at $\eta = 0.06 \sim 0.08$. Analysis on the PM condition for harmonics from Xe shows that L_{coh} for H13, and thus, its intensity gradually increase with η, and peaks around $\eta = 0.06$, which coincides with the dependence of the H27 intensity. If the observed enhancement of H27 from He is solely due to the change of phase-matching, the output signal is expected to be roughly independent of the He gas pressure $[P/(1 + \eta)]$ under the absorption-limited condition. On the other hand, if the DE is a dominant mechanism, the output signal is expected to be proportional to the H13 intensity from Xe or the Xe gas pressure $[\eta P/(1 + \eta)]$. The observed dependence of the H27 intensity on η shown in Fig. 2 supports that the DE effect is mainly responsible for the enhancement seen in Fig. 1, though the addition of the Xe gas affects both the single He atom response (DE) and the propagation effects (PM) in principle.

In summary, we have presented experimental evidence of the DE of He HHG by means of an XUV booster HH from Xe. When the focusing intensity was 1×10^{14} W/cm^2, the harmonic amplified gain was measured to be 4×10^3 at the 27th HH. The spatial and spectral characteristics of the measured HH beam support the fact of the DE process. The experimental results agree well with the direct numerical solution of the TDSE in the SAE approximation. Since the initial tunneling ionization process in the laser field is replaced with a XUV one-photon absorption process [11], the DE is particularly effective when the pump pulse alone hardly ionizes the target gas. Thus, the DE process will be helpful for intracavity HHG by a low-energy pump pulses, such as mode-locked Ti:sapphire femtosecond oscillator pulses with a high repetition rate (>100 MHz), for extending a frequency comb to the XUV region [25,26] without any increase in the pump energy, which promises to lead to another joint frontier of precision spectroscopy and ultrafast science. However, the DE with the mixed gas might be limited since the intracavity schemes with the mixed gas does not allow us to achieve the focusing intensity of $10^{10} \sim 10^{11}$ W/cm^2 for the booster HH with the present state of technology. In addition, the DE process is useful for various applications such as strong-field quantum path control, attosecond control of ionization, and HHG, and attosecond enhancement gate for isolated pulse generation (AEGIS) [27].

This study was financially supported by the Ministry of Education, Culture, Sports, Science, and Technology (MEXT) through a Grant-in-Aid for Scientific Research on Priority Areas for Young Scientists (A) and Young Scientists (B), and a grant from the Research Foundation for Opto-Science and Technology.

*ejtak@riken.jp

[1] M. Hentschel *et al.*, Nature (London) **414**, 509 (2001).
[2] P. Tzallas *et al.*, Nature (London) **426**, 267 (2003).
[3] N. Miyamoto *et al.*, Phys. Rev. Lett. **93**, 083903 (2004).
[4] Y. Nabekawa *et al.*, Phys. Rev. Lett. **94**, 043001 (2005).
[5] M. Drescher *et al.*, Nature (London) **419**, 803 (2002).
[6] T. Sekikawa *et al.*, Nature (London) **432**, 605 (2004).
[7] Y. Nabekawa *et al.*, Phys. Rev. Lett. **96**, 083901 (2006).
[8] Y. Nabekawa *et al.*, Phys. Rev. Lett. **97**, 153904 (2006).
[9] K. J. Schafer *et al.*, Phys. Rev. Lett. **92**, 023003 (2004).
[10] A. D. Bandrauk *et al.*, Phys. Rev. A **66**, 031401 (2002).
[11] K. Ishikawa, Phys. Rev. Lett. **91**, 043002 (2003).
[12] K. L. Ishikawa, Phys. Rev. A **70**, 013412 (2004).
[13] K. Schiessl *et al.*, Phys. Rev. A **74**, 053412 (2006).
[14] E. Takahashi *et al.*, Phys. Rev. A **66**, 021802 (2002).
[15] P. B. Corkum, Phys. Rev. Lett. **71**, 1994 (1993).
[16] J. Biegert *et al.*, Laser Phys. **15**, 899 (2005).
[17] A. Heinrich *et al.*, J. Phys. B **39**, S275 (2006).
[18] E. J. Takahashi *et al.*, IEEE J. Sel. Top. Quantum Electron. **10**, 1315 (2004).
[19] H. G. Muller *et al.*, Phys. Rev. Lett. **81**, 1207 (1998).
[20] H. G. Muller *et al.*, Phys. Rev. A **60**, 1341 (1999).
[21] L. V. Keldysh, Sov. Phys. JETP **20**, 1307 (1965).
[22] A. Rundquist *et al.*, Science **280**, 1412 (1998).
[23] E. Constant *et al.*, Phys. Rev. Lett. **82**, 1668 (1999).
[24] M. V. Amosov *et al.*, Zh. Eksp. Teor. Fiz. **91**, 2008 (1986).
[25] C. Gohle *et al.*, Nature (London) **436**, 234 (2005).
[26] R. J. Jones *et al.*, Phys. Rev. Lett. **94**, 193201 (2005).
[27] K. L. Ishikawa *et al.*, Phys. Rev. A **75**, 021801 (2007).